Geological Survey
of Canada

CURRENT RESEARCH
2002-C26

Geology of the Goldcorp Inc. High Grade zone, Red Lake mine, Ontario: an update

Benoît Dubé, Kenneth Williamson, and M. Malo

2002

Natural Resources Canada
Ressources naturelles Canada

Canada

©Her Majesty the Queen in Right of Canada, 2002
Catalogue No. M44-2002/C26E
ISBN 0-660-18746-9

Available in Canada from the
Geological Survey of Canada Bookstore website at:
http://www.nrcan.gc.ca/gsc/bookstore (Toll-free: 1-888-252-4301)

A copy of this publication is also available for reference by depository libraries across Canada through access to the Depository Services Program's website at http://dsp-psd.pwgsc.gc.ca

Price subject to change without notice

All requests for permission to reproduce this work, in whole or in part, for purposes of commercial use, resale, or redistribution shall be addressed to: Earth Sciences Sector Information Division, Room 402, 601 Booth Street, Ottawa, Ontario K1A 0E8.

Authors' address

B. Dubé *(bdube@nrcan.gc.ca)*
K. Williamson *(kwilliam@nrcan.gc.ca)*
GSC Québec
880 Chemin Sainte-Foy
C.P. 7500
Sainte-Foy, Quebec G1V 4C7

M. Malo *(ess-inrs-mmalo@x1.nrcan.gc.ca)*
INRS-Eau, Terre et Environnement
880 Chemin Sainte-Foy
C.P. 7500
Sainte-Foy, Quebec G1V 4C7

Geology of the Goldcorp Inc. High Grade zone, Red Lake mine, Ontario: an update[1]

Benoît Dubé, Kenneth Williamson, and M. Malo
GSC Québec

Dubé, B., Williamson, K., and Malo, M., 2002: Geology of the Goldcorp Inc. High Grade zone, Red Lake mine, Ontario: an update; Geological Survey of Canada, Current Research 2002-C26, 13 p.

Abstract: Gold mineralization in the Goldcorp Inc. High Grade zone is synchronous with D_2, a protracted event characterized by continuous northeast-southwest-directed shortening. The geometry of the carbonate vein network is related to an early D_{2a} strain increment. D_{2a} has induced folding of the layered sequence and synchronous emplacement of axial-planar fissure veins, bedding-parallel and discordant conjugate veins, and some oblique-lateral displacement that was possibly involved in formation of the carbonate vein network. The main stage of high-grade auriferous silica replacement was contemporaneous with D_2 boudinage of the carbonate veins. The auriferous silica-rich fluid was focused in specific F_{2a} hinge zones because of competence contrast, tangential longitudinal strain, a low-permeability stratigraphic cap, and local higher strain zones. This was followed by a second strain increment (D_{2b}) characterized by attenuation and transposition of the F_{2a} fold limbs, deformation of the vein network, and ultimately reverse-sinistral faulting. Gold was locally remobilized in extremely rich fractures postdating the lamprophyre dykes.

Résumé : La minéralisation aurifère de la zone High-Grade de la société Goldcorp Inc. est contemporaine de la déformation D_2, un épisode de longue durée qui a consisté en un raccourcissement continu, du nord-est vers le sud-ouest. La géométrie du réseau de filons de carbonates est associée à un accroissement précoce D_{2a} de la déformation. D_{2a} a entraîné le plissement de la séquence stratifiée et la mise en place synchrone de fissures de plan axial, de filons parallèles à la stratification et de filons conjugués discordants, ainsi qu'un certain déplacement latéral à composante oblique qui a pu également contribuer à la formation du réseau de filons de carbonates. L'étape principale de remplacement par de la silice à haute teneur en or a été contemporaine du boudinage des filons de carbonates par la déformation D_2. Le fluide riche en silice aurifère s'est concentré dans certaines zones charnières des plis P_{2a} en raison de contrastes de compétence, de la déformation longitudinale tangentielle, de la présence d'horizons stratigraphiques à faible perméabilité et de zones locales d'intense déformation. Un deuxième accroissement de la déformation (D_{2b}) a suivi, et s'est traduit par l'amincissement et la transposition des flancs des plis P_{2a}, par la déformation du réseau filonien et, finalement, par la formation de failles inverses à mouvement senestre. L'or a été remobilisé par endroits au sein de fractures extrêmement riches, dont la formation est postérieure à celle des dykes de lamprophyre.

[1] Contribution to the Western Superior NATMAP Project

INTRODUCTION

The Goldcorp Inc. High Grade zone at the Red Lake mine, one of two mines exploiting the world-class Campbell-Red Lake deposit, is currently the best Canadian example of high-grade gold mineralization. It has (proven and probable) reserves of 1.7 M tonnes grading 69.3 g/t Au (Northern Miner, October 1–7, 2001). Even more impressive is the average grade of 88 g/t Au obtained since gold was first produced (Northern Miner, June 18–24, 2001). It provides an opportunity to define the fundamental geological parameters controlling the formation of high-grade ore and to assist in developing exploration guidelines for such underground high-grade mineralization, a prime target considering the current price of gold as well as environmental regulations for open-pit mining.

In the summer of 2001, we mapped some key localities between levels 31 and 37 of the High Grade zone, a section through the Campbell and Dickenson fault zones on level 16, and some stripped outcrops. This report presents an update on our ongoing study of the Goldcorp Inc. High Grade zone (Dubé et al., 2001a, b).

LOCAL GEOLOGICAL SETTING

Dubé et al. (2001a) and Sanborn-Barrie et al. (2001) describe the regional geological setting; Parker (2000) presents an excellent regional perspective and synthesis of alteration and gold mineralization in the district. Neither subject will be deal with here.

Stratigraphy

The Campbell-Red Lake gold deposit is hosted mainly by Fe-rich tholeiitic basalt and more locally by basaltic komatiite of the Mesoarchean Balmer assemblage. Peridotite komatiite, variolitic basalt, rhyolite, mafic intrusions, and synvolcanic sedimentary rocks complete this assemblage in the mine sequence (Penczak and Mason, 1997). To the southeast, pre-2745 Ma Huston polymictic conglomerate unconformably overlies the Balmer assemblage (Sanborn-Barrie et al., 2001). The host rocks at the Red Lake mine have been contact metamorphosed to amphibolite facies, as a result of emplacement of the nearby Walsh Lake Pluton (marginal phase of the Trout Bay Batholith) (Damer, 1997).

Structure

Geophysical surveys and local outcrops reveal the presence of an open, north-trending, large-scale F_1 fold (MacGeehan and Hodgson, 1982; M. O'Dea, unpub. rept., 1999; Sanborn-Barrie et al., 2000). Mine-sequence rocks trend approximately east and dip south; however, to the east, all units have been folded by southeast-trending and southeast-plunging (~60°) F_{2a} folds, forming antiform-synform pairs (Fig. 1, 2). These folds are transected by the Campbell and Dickenson faults, two steeply dipping (70–80°S), southeast-trending, subparallel structures that can be traced over 1500 m along strike and coincide with the transposed limbs of the F_{2a} folds (*see* Dubé et al., 2001a, Fig. 1). These faults coincide spatially with a large proportion of the ore zones in the deposit. From the apparent rock displacements, the Campbell and Dickenson fault zones have been interpreted as a sinistral strike-slip fault and a dextral strike-slip fault (Mathieson, 1982; Penczak and Mason, 1997) respectively, or as an imbricated, reverse-sinistral fault system (M. O'Dea, unpub. rept., 1999). In an unpublished report (2001), N. Archibald and V. Wall have recently interpreted a sinistral fault, the 'Red Lake Fault', parallel to the Campbell and Dickenson faults and southeast of the latter. It has an apparent sinistral displacement of 800 m and connects basaltic komatiite at the Campbell and Dickenson mines. In the High Grade zone area, it may coincide with the footwall shear zone (Fig. 1a).

Campbell Fault zone

The Campbell Fault is exposed on level 16 of the Red Lake mine and defines the contact between the peridotite komatiite of the footwall and the basalt of the hanging wall (Fig. 3a). Deformation of the peridotite komatiite is heterogeneous and characterized by high-strain zones a few metres to tens of metres wide in which intense ductile deformation alternates with lower strain domains. These high-strain zones are located up to 150 m away in the footwall of the Campbell Fault. The ultramafic rocks are transformed into talc-chlorite schist and local mylonite characterized by a penetrative, southeast-trending S_2 foliation with local, foliation-parallel, extensional carbonate veinlets. Local C-S-type fabrics within these high-strain zones suggest a reverse component of shearing. Outside these high-strain corridors, a relatively weak S_2 foliation is present with minor foliation-parallel veinlets. Toward the Campbell Fault, the peridotite komatiite contains abundant, millimetre-wide, foliation-parallel, extensional, sheeted carbonate veinlets. In the vicinity of the fault, both the veinlets and the foliation are folded by a westerly plunging, open F_{2b} fold with northeast vergence, compatible with a reverse component of motion along the Campbell Fault. In the immediate footwall of the fault, the sheeted veinlets are brecciated. The fault plane itself is oriented 110°/54° and corresponds to a discrete, centimetre-wide surface that cuts across the steeper S_2 fabric and locally dragged or cut carbonate veinlets (Fig. 3a). The fault zone is also characterized by local, C-S-type fabrics, indicating a reverse component of motion (Fig. 3b) with a significant sinistral component (up to 500–600 m), on the basis of lateral rock displacements (Dubé et al., 2001a, Fig. 1). The Campbell Fault postdates carbonate alteration and mineralization, but occurred early during feldspar porphyry dyke emplacement as these dykes cut across the hydrothermal corridor, but do not appear to have been significantly displaced by the reverse-sinistral motion.

The basalt in the hanging wall is moderately foliated (S_2) and contains a very large number of iron-carbonate extensional and breccia veins and much associated carbonatization of the host basalt. This zone corresponds to a hydrothermal corridor with abundant Fe-carbonate veins and local wall-rock replacement ore (Fig. 3c, d). Two main sets of

extensional carbonate veins are present within the basalt; one set, of centimetre-wide, sheeted veins with local carbonate fibres, is subparallel to S_2 (125°/67°) and a second set, with colloform-cockade textures, is oriented on average 153°/57°. These veins are buckled, clearly indicating that they are pre- to early S_2 foliation. Carbonate veinlets and host basalt carbonatization become more abundant toward the ESC ore zone farther in the hanging wall toward the south.

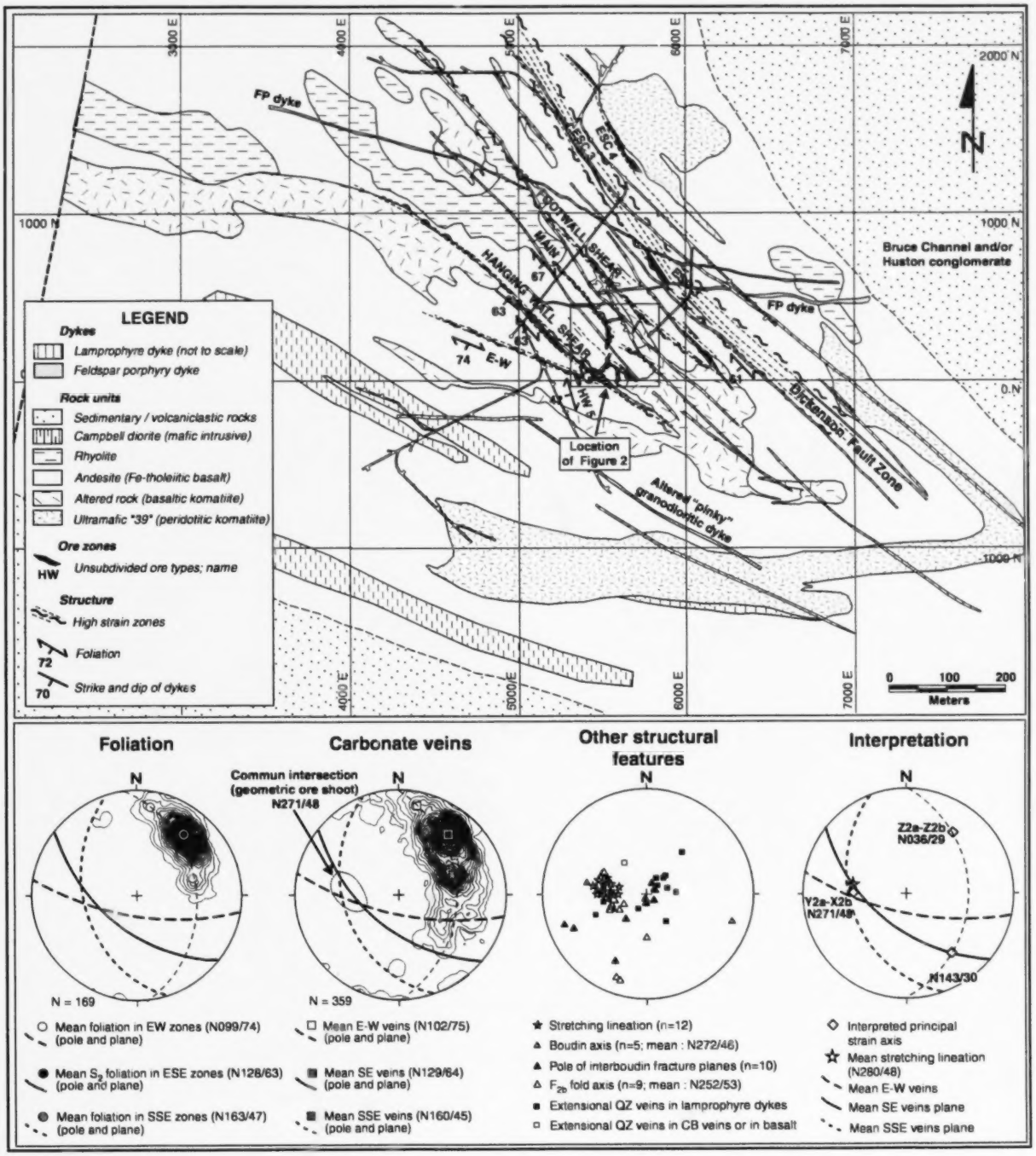

Figure 1. *Geology of 34 level, Red Lake mine* (modified from *Goldcorp Inc. geological data; grid in feet) and stereographic projections of the main structural features of the Red Lake deposit (equal area projection, lower hemisphere).*

RED LAKE MINE TREND

The Campbell, Dickenson, and Red Lake faults are developed within a CO_2-rich hydrothermal corridor that coincides spatially with most of the ore zones. The flattened F_{2a} folds with highly strained limbs, the southeast-trending faults, and the associated corridor of alteration and mineralization define a southeast-trending structural lineament known as the 'Cochenour-Gullrock Lake deformation zone' (Andrews et al., 1986) or the 'Red Lake mine trend'. This Red Lake mine trend lineament is traced from the Campbell-Red Lake deposit northwest at least to the Cochenour mine (*see* Sanborn-Barrie et al., 2001) and corresponds to a zone of heterogeneous, protracted D_2 strain.

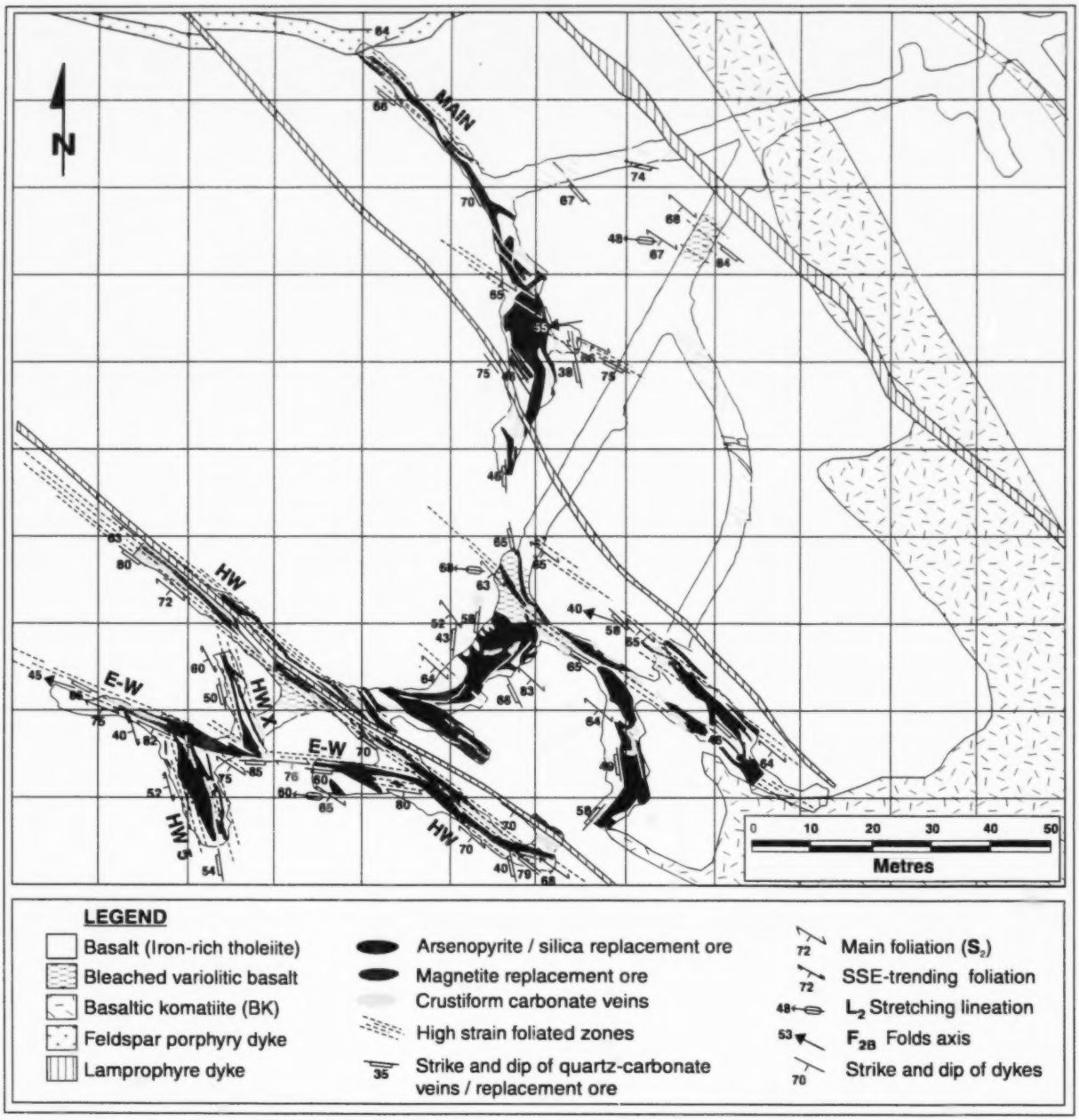

Figure 2. *Detailed geology of the High Grade zone, 34 level, cuts 2 and 4* (modified from *Goldcorp Inc. geological data; 50 feet grid).*

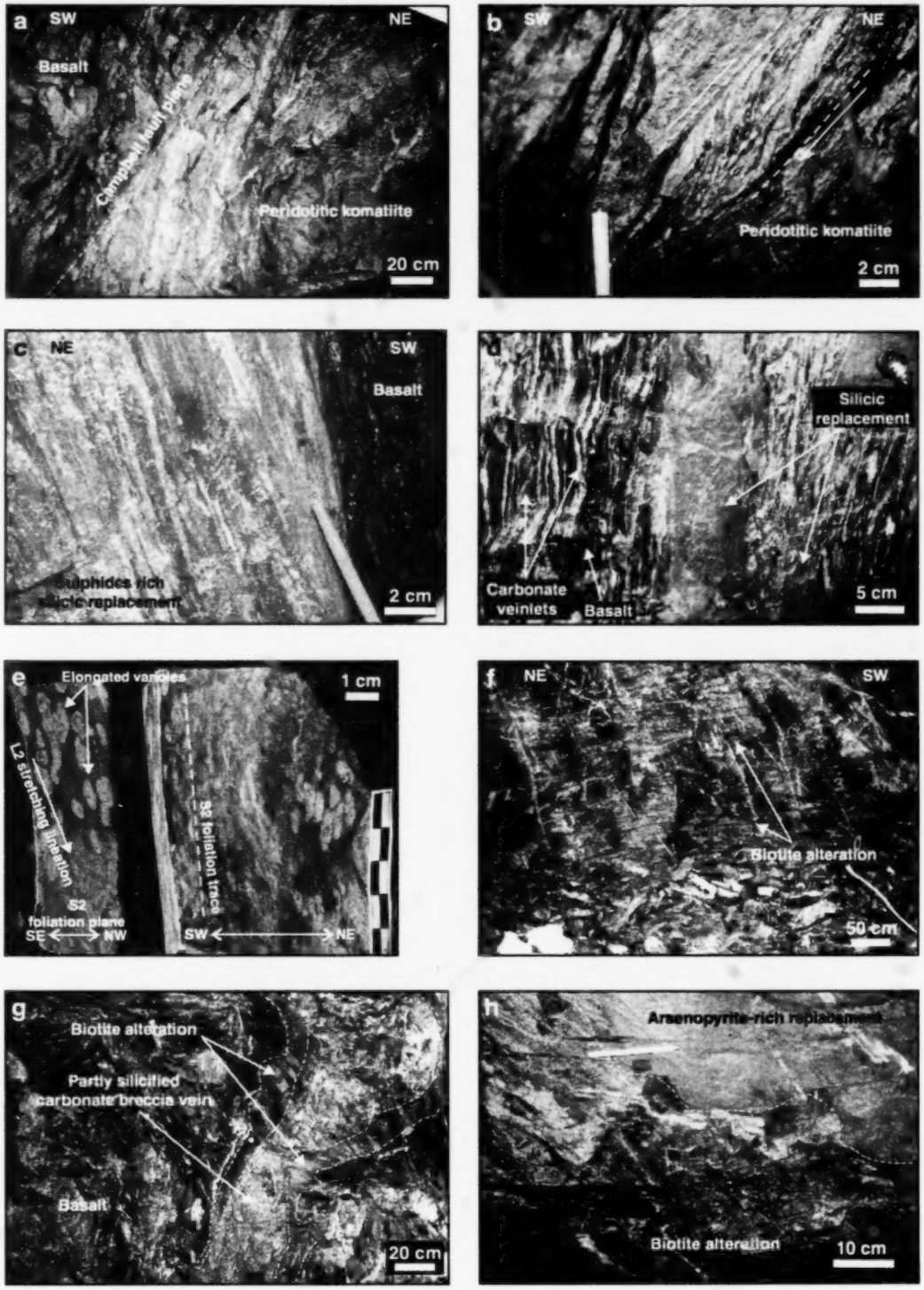

Figure 3. *a) Campbell Fault, section view; b) C-S-type fabric along the Campbell Fault, section view; c) ESC-style sulphide rich silicic replacement of carbonatized basalt, section view; d) sulphide-rich silicic replacement of carbonatized basalt, back view; e) elongated varioles in bleached basalt; f) section view showing reddish-brown biotite-carbonate alteration; g) symmetrical distribution of biotite-carbonate alteration next to a silicified carbonate vein, section view; h) alteration front of arsenopyrite and quartz replacing biotite-carbonate alteration.*

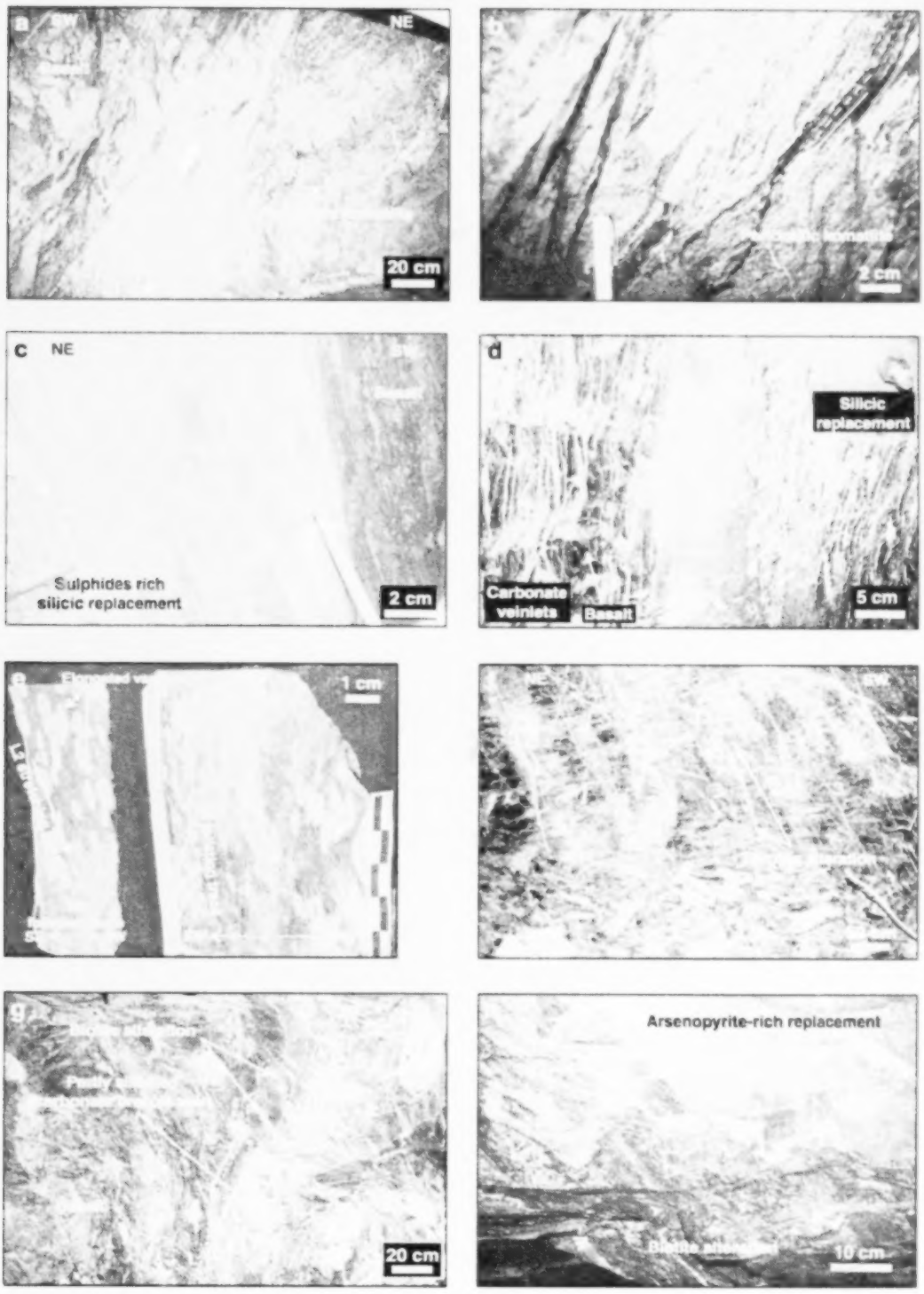

Figure 3. *a) Campbell Fault, section view; b) C-S-type fabric along the Campbell Fault, section view; c) ESC-style sulphide-rich silicic replacement of carbonatized basalt, section view; d) sulphide-rich silicic replacement of carbonatized basalt, back view; e) elongated varioles in bleached basalt; f) section view showing reddish-brown biotite-carbonate alteration; g) symmetrical distribution of biotite-carbonate alteration next to a silicified carbonate vein, section view; h) alteration front of arsenopyrite and quartz replacing biotite-carbonate alteration.*

Detailed work at different locations within the Red Lake mine trend, particularly on stripped outcrops near the Cochenour mine headframe, indicates that D_2 strain is moderate overall and dominated by southeast-trending, S_2-cleavage, axial-planar to westerly plunging F_2 folds. S_2 contains a relatively steep westerly plunging L_2 stretching lineation (Sanborn-Barrie et al., 2001). D_1 is characterized by bedding-parallel S_1 foliation. Many carbonate veins and carbonatized zones are folded, crenulated, and/or transposed by S_2, suggesting that they are pre- to early D_2 structures (*also* Parker, 2000). The Red Lake mine trend is also characterized by many brittle faults known as 'black line faults', which are barren, millimetre wide, and filled by tourmaline and locally by quartz. They commonly trend east to southeast and cut across the alteration and ore zones and the feldspar porphyry dykes with respectively a dextral and sinistral component of displacement over centimetres to a few metres. Locally, they form complex corridors (≤1 m) of multiple Riedel-type slip planes cutting the ore. Some brittle structures are locally crenulated by the S_2 foliation, suggesting that they are syn- to late ((?)post)-D_2 structures.

D zone

ESC replacement ore (Rogers, 1992) was visited on several levels and mapped on level 16 in the hanging wall of the Campbell Fault. There the 'D zone', a mineralized zone within the Campbell Fault zone corridor, is exposed over a few metres. It is hosted by foliated, carbonatized basalt containing 40% to 60% foliation-parallel (122°/70°) and locally buckled, foliation-oblique, extensional Fe-carbonate veins and breccia. The mineralized zone is one of replacement and is characterized by silicification and sulphidization superposed on carbonatized basalt (Fig. 3c, d). It contains 5% to ≤15% very fine-grained sulphides, mainly pyrite and pyrrhotite with arsenopyrite and local stibnite. Some pyrite layers are 5 mm to 1 cm wide, parallel to and replacing the Fe-carbonate veinlets. The mineralized zone is slightly discordant with respect to the steeper S_2 foliation. The D zone has an alteration style (silicification, arsenopyrite) and chronology (post-carbonate veining) similar to those in the High Grade zone. The main differences are the structural location and the extremely rich ore in the High Grade zone.

GOLDCORP INC. HIGH GRADE ZONE

The Goldcorp Inc. High Grade zone is currently defined and mined between levels 31 and 37. It is characterized by multi-ounce ore zones located within or near an F_{2a} antiform hinge zone and is almost totally hosted by Fe-tholeiitic basalt near the contact with the basaltic komatiite (Fig. 1a, 2). These ore zones have a known extent of ~130 m laterally and at least 400 m vertically. The F_{2a} antiform is defined by the geometry of rhyolite units northwest of and the basalt–basaltic komatiite contact southeast of the High Grade zone (Fig. 1a); it is responsible for the apparent thickening of the basalt in the hinge zone. These F_{2a} folds are flattened and their limbs commonly transposed and/or transected by metre-wide, southeast-trending, high-strain zones or by the Dickenson, Campbell, and Red Lake faults.

All these units are cut by feldspar porphyry and lamprophyre dykes (Fig. 1a, 2). The feldspar porphyry dykes trend northwest to east to southeast and cut high-grade ore. Locally, they are moderately foliated by S_2, although they cut across both F_{2a} fold limbs. On level 34, the footwall shear zone, a D_2 structure cuts such a dyke with 7 to 8 m of sinistral displacement. Thus, the feldspar porphyry dykes are post-F_{2a} folds, but late D_2.

Three sets of lamprophyre dykes are present; one is subparallel to S_2 (130°/70°), another trends east and dips steeply, and a third strikes north and dips shallowly west (Fig. 1a). The steeply dipping lamprophyre dykes cut the high-grade ore and the feldspar porphyry dykes with apparent sinistral displacement.

Structure, veins, and ore zones

Figure 2 shows the High Grade zone as mapped on level 34 (cuts 2–4). The S_2 foliation represents the main fabric developed in the basalt defining local, centimetre- to metre-wide, southeast-trending (128°/63°), high-strain zones, which coincide with high-grade mineralization and alteration. S_2 locally contains a westerly plunging L_2 stretching lineation (280°/48°) (Fig. 1d, 3e). Both flattened limbs of the F_{2a} antiform are transposed by ductile high-strain zones, known as the 'southeast-trending footwall' and the 'east-trending east-west shears' (Fig. 1a). The hanging-wall shear is a high-strain zone axial planar to the F_{2a} fold and transecting the hinge area (Fig 1a, 2). Two other sets of smaller subsidiary high-strain zones are present southwest of the hanging-wall shear. The steeply south-dipping subsidiary east-west shear (Fig. 2) is 3 to 4 m wide and characterized by a well developed foliation trending 099°/74°. It is well mineralized and can be traced westward over 100 m. To the east it merges with the hanging-wall shear. This east-west high-strain zone cuts a west-dipping, south-southeast-trending (~163°/47°), high-strain zone (zone HW5), with an apparent dextral offset (Fig. 2). Zone HW5 accounts for one quarter of the reserves and has a known vertical extent of at least 650 m, the most extensive among the high-grade structures. It and the hanging-wall shear could well be the most important High Grade zone feeders tapping deeper sources and allowing the upward migration of high-grade auriferous fluid in the low-pressure F_{2a} fold nose.

These three sets of higher strain zones host foliation-parallel and -oblique, extensional, barren, carbonate-sheeted veins that are extensively developed in the basalt, but also locally present in the rhyolite and basaltic komatiite. Within a given higher strain zone, most veins are subparallel to the host structure, although the two other vein sets may be present to a lesser degree.

The southeast-trending carbonate veins are subparallel to S_2 foliation (129°/64°). They are the most common set, forming sheeted fissure veins with well developed colloform-crustiform banding and breccia. A second set of veins is less abundant and corresponds to colloform-crustiform veins similar to the first set, but oblique to S_2 and cut by the main southeast-trending set. They strike south-southeast (160°/45°), and are

subparallel to and enclosed within structures such as HW5. Some of them locally contain carbonate fibres perpendicular to banding and/or vein walls. A subgroup of this south-southeast-striking set corresponds to large carbonate breccia and cavity-fill veins with a slightly shallower dip (166°/43°). They form large, spectacular breccia veins, up to 8 to 10 m wide, with centimetre- to metre-long angular wall-rock fragments, colloform-crustiform banding, and cockade texture (*see* Dubé et al., 2001a). A third set is enclosed within and subparallel to the east-trending structures (102°/75°).

Locally, the high-grade ore zones gradually change orientation from southeast to south-southwest closer to the contact with the basaltic komatiite; this is attributed to competence contrasts and strain refraction (Fig. 2). Gold-bearing, metre-wide, east-west shear zones (090°/65°) are locally developed in the ultramafic rocks close to and parallel to the basalt contact.

All these southeast-, east-, and south-southeast-trending structures intersect each other at approximately 275°/45° (Fig. 1c). This intersection defined and controlled spectacular geometric ore shoots characterized by intense silicification with abundant arsenopyrite (Dubé et al., 2001a; N. Archibald and V. Wall, unpub. rept., 2001). It is colinear with the L_2 lineation and the F_{2b} fold axis deforming the carbonate veins (Fig. 1d).

All the carbonate veins and ore zones have been deformed to varying degrees. The different sets of carbonate veins and ore zones hosted by centimetre- to metre-scale, S_2-foliated zones and high-strain zones underwent boudinage with antithetically rotated, asymmetrical pull-aparts or back-rotated vein segments enclosed in foliated (S_2) basalt. The asymmetry of the boudins is compatible with a reverse component of motion (Dubé et al., 2001a). The elongation axis of the boudins plunges southwest (Fig. 1d). Many veins oblique to S_2 are commonly folded by southwest-plunging F_{2b} folds, a second generation of D_2-related folding. Folded carbonate veins with boudinaged limbs are common. This suggests that the boudinage is contemporaneous with folding, explaining the parallelism between the elongation axis of boudins and F_{2b} fold axes (Fig. 1d).

West-southwest-plunging striations (254°/28°) with steps developed on foliation planes and lamprophyre dyke walls indicate a late, oblique, sinistral-reverse sense of motion.

Alteration

The high-grade ore zones were formed by silicic replacement of carbonate colloform-crustiform and breccia veins and enclosing wall rock (Dubé et al., 2001a). The alteration developed in the host basalt is commonly associated with increasing strain toward the ore zone.

Different alteration assemblages occur in the Red Lake mine and have been interpreted as metamorphic products of near-surface hydrothermal alteration (Penczak and Mason, 1997, 1999; Damer, 1997). In the Goldcorp Inc. High Grade zone, at least three alteration facies are present, 1) an outer, metre-wide, garnet-chlorite-magnetite alteration with chlorite-amphibole-andalusite and locally associated centimetre- to metre-wide 'bleached zone' containing andalusite-muscovite-quartz-ilmenite (Damer, 1997) and especially well developed in variolitic basalt; 2) a proximal, centimetre- to metre-wide, massive to laminated, reddish-brown, biotite-carbonate alteration with disseminated pyrite (3–5%) and carbonate veinlets in well foliated basalt (Fig. 3f, g); and 3) a gold-rich, strongly foliated, silicified zone with abundant fine-grained arsenopyrite, sericite, and rutile, and lesser amounts of pyrite, pyrrhotite, magnetite, and stibnite (≤15%). This third alteration facies is adjacent to the silicified auriferous carbonate veins and replaces the biotite-carbonate-rich alteration (Fig. 3h, 4a). Gold-bearing silicic replacement and arsenopyrite-rich selvages commonly occur along the margins of the carbonate veins in varied intensity. The biotite-carbonate and silicic alteration facies replace wall-rock clasts within the carbonate breccia veins. The reddish-brown biotite-carbonate alteration could be symmetrically distributed on both sides of the silicified ore veins (Fig. 3g). However, these alteration facies are commonly better developed in the footwall of the silicified carbonate vein, which is typically cut by numerous carbonate veins, whereas the hanging-wall contact of the ore vein is commonly marked by a sharp rectilinear contact potentially due to faulting (Fig. 4b). The arsenopyrite is directly associated with high-grade gold and is essentially related to the silicic replacement of the vein and host rocks. Where there is no silicification, there is no arsenopyrite (Fig. 4g, h). Spectacular semimassive, arsenopyrite-rich ore zones occur at the intersection of the different sets of veins and structures and define west-plunging, geometric, high-grade ore shoots parallel to their line of intersection. In the ultramafic rocks, the alteration is typified by abundant Fe-Mg-carbonate with green micas. The carbonatized ultramafic rocks are less reactive to the silicic fluid, probably because the fluid is highly buffered by high CO_2 content and also because the fluid–rock ratio is smaller.

Hydrothermal magnetite occurs locally within the hinge of folded carbonate veins and is common in the matrix of silicified carbonate breccia veins within the ore zone. Barren magnetite breccia is locally cut by high-grade ore or cuts arsenopyrite-rich replacement ore. These crosscutting relationships suggest that all are broadly contemporaneous or that several generations of hydrothermal magnetite are present. Magnetite occurs in the auriferous east-west shear structure, especially toward the external limit of the High Grade zone (Fig. 2) where it may represent a change from distal oxidized (magnetite-rich) to proximal reducing (arsenopyrite-rich) conditions in the zone, as proposed by N. Archibald and V. Wall (unpub. rept., 2001).

A key alteration vector for the high-grade mineralization is the presence of the reddish-brown biotite-carbonate alteration developed in the basalt that indicates proximity of potential high-grade ore (Fig. 3c, d). This alteration is commonly associated with silicification of the carbonate vein and is the most proximal alteration to the ore-bearing siliceous and arsenopyrite-rich replacement of the carbonate veins and host rocks (Fig. 3e, f).

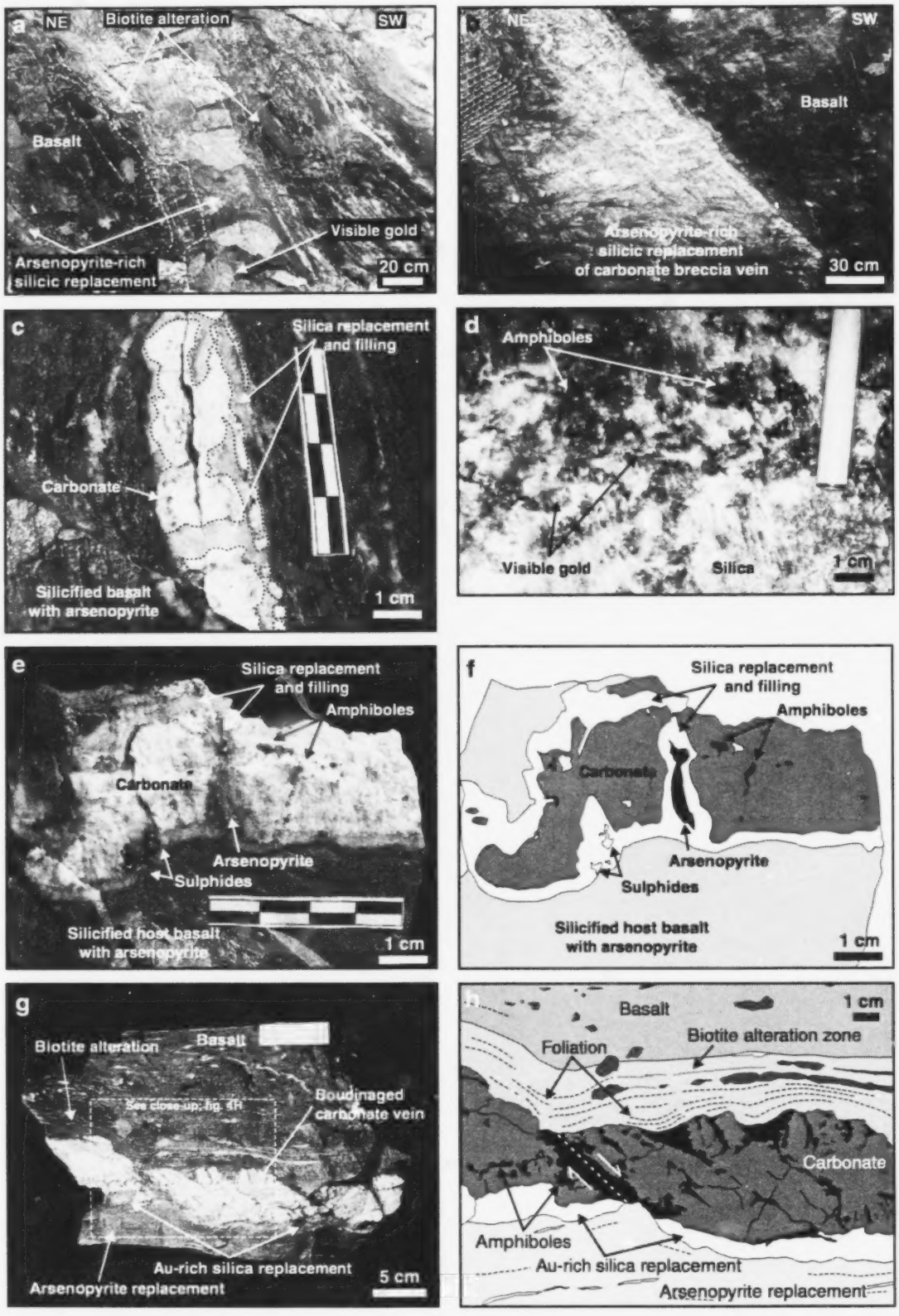
a
NE
Biotite alteration
SW
Basalt
Visible gold
Arsenopyrite-rich
silicic replacement
20 cm
b
NE
SW
Basalt
Arsenopyrite-rich
silicic replacement
of carbonate breccia vein
30 cm
c
Silica replacement
and filling
Carbonate
Silicified basalt
with arsenopyrite
1 cm
d
Amphiboles
Visible gold
Silica
1 cm
e
Silica replacement
and filling
Amphiboles
Carbonate
Arsenopyrite
Sulphides
Silicified host basalt
with arsenopyrite
1 cm
f
Silica replacement
and filling
Amphiboles
Carbonate
Arsenopyrite
Sulphides
Silicified host basalt
with arsenopyrite
1 cm
g
Biotite alteration
Basalt
See close-up, fig. 4h
Boudinaged
carbonate vein
Au-rich silica replacement
Arsenopyrite replacement
5 cm
h
Basalt
1 cm
Biotite alteration zone
Foliation
Carbonate
Amphiboles
Au-rich silica replacement
Arsenopyrite replacement

Chronology of gold replacement

The chronology of the gold-rich silicic replacement is one of the most critical elements for understanding the formation of the High Grade zone. Dubé et al. (2001a) described evidence for multiple stages of gold deposition, silicic replacement, and carbonate veining, and showed that the main gold-bearing silicic replacement of the carbonate veins was syn- or post-development of the D_2 asymmetrical boudins. New observations support this interpretation. The pull-aparts between some of the partly silicified carbonate boudins are filled by gold-bearing quartz (Fig. 4c) or by auriferous quartz and arsenopyrite (Fig. 4e, f). However, Figures 4g and 4h show a silicified carbonate vein in which both the carbonate and the gold-rich silicified zone show boudinage with amphibole in the pull-apart. Visible gold also occurs directly hosted by amphibole within a silicified carbonate vein (Fig. 4d). Alternatively, some silicified carbonate veins and associated arsenopyrite-rich alteration selvages are deformed or folded by the S_2 fabric, indicating that at least part of the D_2 strain has affected the high-grade ore. These observations, combined with those of Dubé et al. (2001a), suggest that the main stage of high-grade, Au-rich silica and arsenopyrite was contemporaneous with the D_2 boudinage of the carbonate veins. They suggest a progressive and dynamic syn-D_2 mineralization event dominated by silicification of carbonate veins with locally some late gold-bearing or barren colloform carbonate veining cutting across the high-grade silicic replacement ore and ESC-style wall-rock replacement ore.

Remobilization

Late- to post-D_2 strain and metamorphism have partly remobilized gold from the main stage of silicic mineralization into late fractures to produce extremely rich ore zones with spectacular visible gold (Dubé et al., 2001a, b). Remobilization is suggested by visible gold present in the hinge of a small-scale F_{2b} fold nose deforming a silicified carbonate vein on level 37, and by gold coating shallow-dipping late fractures at high angle to S_2. Remobilization is demonstrated by visible gold filling or coating fractures present within a steeply dipping post-ore lamprophyre dyke (Fig. 5). The dyke is undergoing U-Pb dating and will provide a maximun age for the remobilization.

Figure 4. ***a)*** *High-grade arsenopyrite-rich silicic replacement of reddish-brown biotite-carbonate alteration of host basalt, section view;* ***b)*** *silicifed carbonate breccia vein, section view;* ***c)*** *silica replacement and filling of a boudinaged carbonate vein (photograph courtesy of Goldcorp Inc.);* ***d)*** *visible gold within amphiboles in a silicified carbonate breccia vein;* ***e)*** *partly silicified boudinaged carbonate vein with silica and arsenopyrite filling spaces between boudins;* ***f)*** *sketch of* ***e****;* ***g)*** *asymmetrical boudinage of a silicified carbonate vein;* ***h)*** *sketch of* ***g****.*

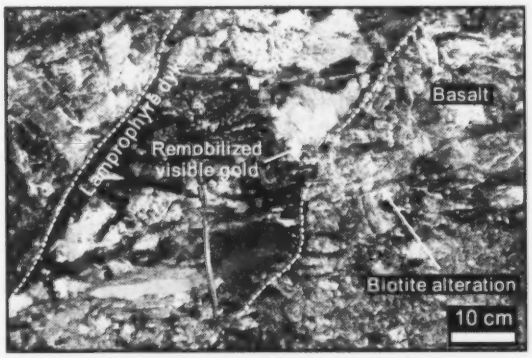

Figure 5. *Remobilized gold coating and filling fractures cutting across a steeply dipping lamprophyre dyke, section view (*from *Dubé et al., 2001b).*

DISCUSSION

The spatial relationships between abundance and thickness of carbonate veins, high-grade ore zones, and F_{2a} fold hinge deforming the basalt–ultramafic rock contact indicate that the F_{2a} fold exerted geological control on the formation of the Goldcorp High Grade zone (Dubé et al., 2001a) and on other zones such as the L zone at Campbell. The carbonate fissure veins are more abundant and thicker within the fold nose, and the auriferous silica-rich fluid was focused into those lower pressure F_{2a} hinge areas because of several factors, including competence contrast between basalt and ultramafic rocks, tangential longitudinal strain associated with F_{2a} folds inducing layer-parallel stretching in the more rigid basalt close to the basaltic komatiite, and southeast-trending higher strain zones associated with fold tightening and limb transposition due to continuous northeast-southwest shortening. Dubé et al. (2001a) also proposed that the carbonatized ultramafic rocks acted as a mechanically less permeable barrier controlling fluid migration along or near the contact with the folded basalt, thus allowing a buildup of supralithostatic fluid pressure, enhancing the dilation and formation of axial-planar fissures and oblique veins, and inducing a ponding effect in the underlying basalt by trapping the fluid. Such a ponding effect is also locally developed within ESC ore close to the contact with folded ultramafic rocks on level 23. Figures 6a and 6b show a vein distribution elsewhere in the Red Lake mine trend similar to the vein pattern in the Campbell-Red Lake deposit. The veins are controlled by layer-parallel stretching of a folded (F_2) stiff layer, with thicker extensional fissure veins in the outer arc and at a high angle to the folded competent layer and buckled bedding-parallel veins along the competent–incompetent interface. Discordant veins also formed along one of the flattened fold limbs. This illustrates that folding, layer anisotropy, and incremental shortening could in large part explain the vein geometry of the deposit. Continuous shortening of the folded layered sequences in the deposit will ultimately result in shearing of the limbs, deformation of the

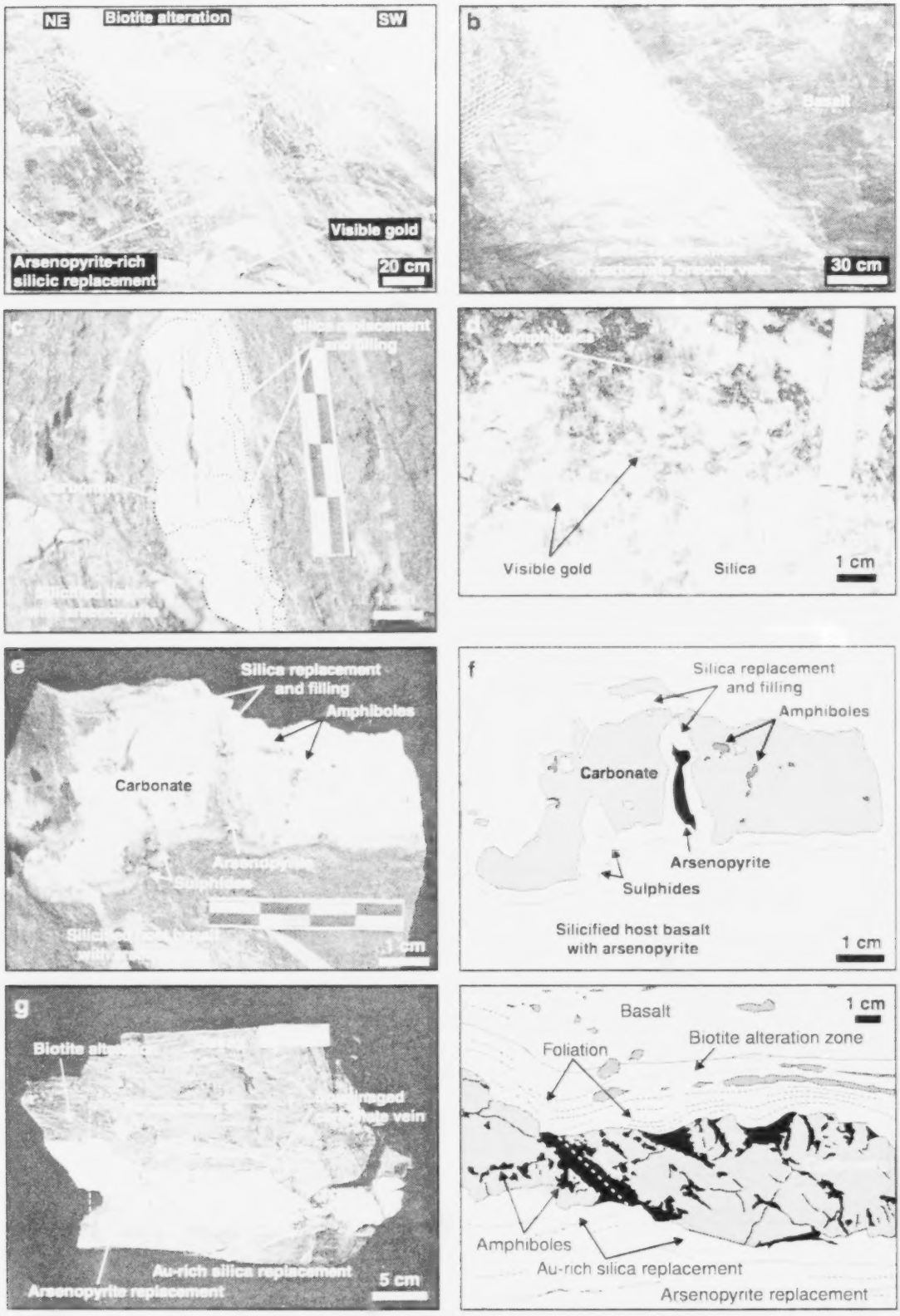
NE
Biotite alteration
SW
Visible gold
Arsenopyrite-rich
silicic replacement
20 cm
b
30 cm
Visible gold
Silica
1 cm
e
Silica replacement
and filling
Amphiboles
Carbonate
f
Silica replacement
and filling
Amphiboles
Carbonate
Arsenopyrite
Sulphides
Silicified host basalt
with arsenopyrite
1 cm
g
Au-rich silica replacement
Arsenopyrite replacement
5 cm
Basalt
1 cm
Biotite alteration zone
Foliation
Amphiboles
Au-rich silica replacement
Arsenopyrite replacement

Chronology of gold replacement

The chronology of the gold-rich silicic replacement is one of the most critical elements for understanding the formation of the High Grade zone. Dubé et al. (2001a) described evidence for multiple stages of gold deposition, silicic replacement, and carbonate veining, and showed that the main gold-bearing silicic replacement of the carbonate veins was syn- or post-development of the D_2 asymmetrical boudins. New observations support this interpretation. The pull-aparts between some of the partly silicified carbonate boudins are filled by gold-bearing quartz (Fig. 4e) or by auriferous quartz and arsenopyrite (Fig. 4e, f). However, Figures 4g and 4h show a silicified carbonate vein in which both the carbonate and the gold-rich silicified zone show boudinage with amphibole in the pull-apart. Visible gold also occurs directly hosted by amphibole within a silicified carbonate vein (Fig. 4d). Alternatively, some silicified carbonate veins and associated arsenopyrite-rich alteration selvages are deformed or folded by the S_2 fabric, indicating that at least part of the D_2 strain has affected the high-grade ore. These observations, combined with those of Dubé et al. (2001a), suggest that the main stage of high-grade, Au-rich silica and arsenopyrite was contemporaneous with the D_2 boudinage of the carbonate veins. They suggest a progressive and dynamic syn-D_2 mineralization event dominated by silicification of carbonate veins with locally some late gold-bearing or barren colloform carbonate veining cutting across the high-grade silicic replacement ore and ESC-style wall-rock replacement ore.

Remobilization

Late- to post-D_2 strain and metamorphism have partly remobilized gold from the main stage of silicic mineralization into late fractures to produce extremely rich ore zones with spectacular visible gold (Dubé et al., 2001a, b). Remobilization is suggested by visible gold present in the hinge of a small-scale F_{2b} fold nose deforming a silicified carbonate vein on level 37, and by gold coating shallow-dipping late fractures at high angle to S_2. Remobilization is demonstrated by visible gold filling or coating fractures present within a steeply dipping post-ore lamprophyre dyke (Fig. 5). The dyke is undergoing U-Pb dating and will provide a maximun age for the remobilization.

Figure 4. ***a****) High-grade arsenopyrite-rich silicic replacement of reddish-brown biotite-carbonate alteration of host basalt, section view;* ***b****) silicified carbonate breccia vein, section view;* ***c****) silica replacement and filling of a boudinaged carbonate vein (photograph courtesy of Goldcorp Inc.);* ***d****) visible gold within amphiboles in a silicified carbonate breccia vein;* ***e****) partly silicified boudinaged carbonate vein with silica and arsenopyrite filling spaces between boudins;* ***f****) sketch of* ***e****;* ***g****) asymmetrical boudinage of a silicified carbonate vein;* ***h****) sketch of* ***g****.*

Figure 5. *Remobilized gold coating and filling fractures cutting across a steeply dipping lamprophyre dyke, section view (from Dubé et al., 2001b).*

DISCUSSION

The spatial relationships between abundance and thickness of carbonate veins, high-grade ore zones, and F_{2a} fold hinge deforming the basalt–ultramafic rock contact indicate that the F_{2a} fold exerted geological control on the formation of the Goldcorp High Grade zone (Dubé et al., 2001a) and on other zones such as the L zone at Campbell. The carbonate fissure veins are more abundant and thicker within the fold nose, and the auriferous silica-rich fluid was focused into those lower pressure F_{2a} hinge areas because of several factors, including competence contrast between basalt and ultramafic rocks, tangential longitudinal strain associated with F_{2a} folds inducing layer-parallel stretching in the more rigid basalt close to the basaltic komatiite, and southeast-trending higher strain zones associated with fold tightening and limb transposition due to continuous northeast-southwest shortening. Dubé et al. (2001a) also proposed that the carbonatized ultramafic rocks acted as a mechanically less permeable barrier controlling fluid migration along or near the contact with the folded basalt, thus allowing a buildup of supralithostatic fluid pressure, enhancing the dilation and formation of axial-planar fissures and oblique veins, and inducing a ponding effect in the underlying basalt by trapping the fluid. Such a ponding effect is also locally developed within ESC ore close to the contact with folded ultramafic rocks on level 23. Figures 6a and 6b show a vein distribution elsewhere in the Red Lake mine trend similar to the vein pattern in the Campbell–Red Lake deposit. The veins are controlled by layer-parallel stretching of a folded (F_2) stiff layer, with thicker extensional fissure veins in the outer arc and at a high angle to the folded competent layer and buckled bedding-parallel veins along the competent–incompetent interface. Discordant veins also formed along one of the flattened fold limbs. This illustrates that folding, layer anisotropy, and incremental shortening could in large part explain the vein geometry of the deposit. Continuous shortening of the folded layered sequences in the deposit will ultimately result in shearing of the limbs, deformation of the

earlier vein network, (?) emplacement of some new veins, and formation or reactivation of late- to post-mineralization faults such as the Campbell Fault.

Although best developed in the fold nose, southeast-, east-, and south-southeast-trending veins with similar orientations are observed in fold positions other than the hinge area, such as within the limbs or the hydrothermal corridor representing the zone delimited by the Campbell and Dickenson faults (*see* Dubé et al., 2001a, Fig. 1), thus in areas where layer-parallel extension of competent layers in the fold hinges cannot be as easily invoked. Figures 1b and 1c show that in the Goldcorp High Grade zone, the poles of foliation and veins fall on a great circle with a pole corresponding to the axes of folds deforming the veins. This distribution of poles is not solely the product of folding of the main S_2 fabric and subparallel veins, as it may appear at first glance. Although it is partly due to folded veins, it largely reflects the presence of several vein sets intersecting along a line parallel to F_{2b} fold axes, as illustrated by maxima on the stereonets (Fig. 1c) and as recognized elsewhere in the deposit by Rogers (1992) and Zhang et al. (1997). Although the original vein geometry has been modified by continuous deformation, the three main sets of carbonate veins are interpreted to form a broadly contemporaneous, three-dimensional network with the southeast set being by far the best developed. This vein network developed mainly during the same deformation increment, as suggested by the identical hydrothermal

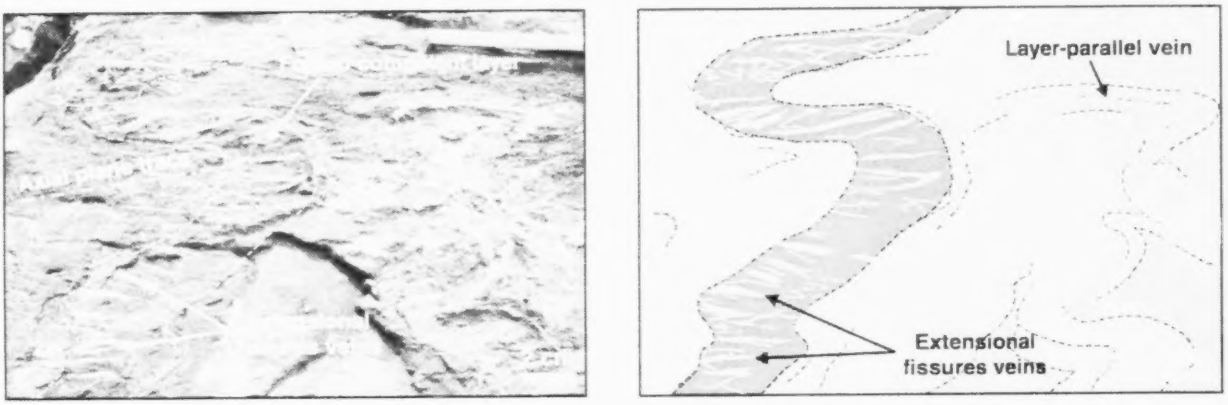

Figure 6. *a) Small-scale example of vein distribution controlled by layer-parallel stretching of a folded (F_2) stiff layer, with thicker extensional fissure veins in the outer arc and at a high angle to the folded competent layer and buckled bedding-parallel veins along the competent–incompetent interface, plane view; **b**) sketch of **a**.*

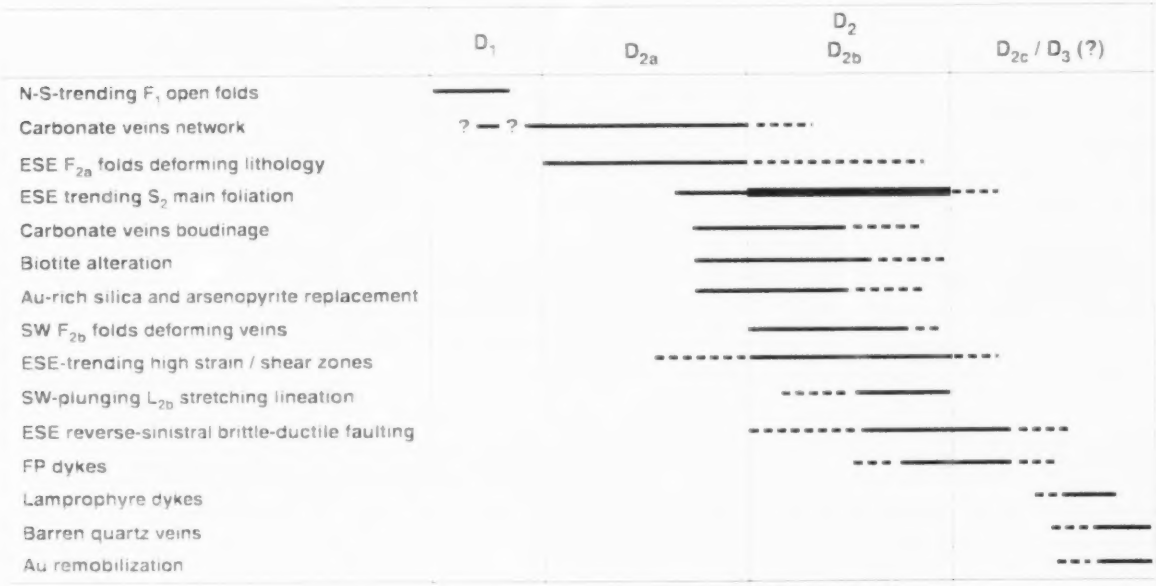

Figure 7. Relative chronology of the main geological features.

earlier vein network, (?) emplacement of some new veins, and formation or reactivation of late- to post-mineralization faults such as the Campbell Fault.

Although best developed in the fold nose, southeast-, east-, and south-southeast-trending veins with similar orientations are observed in fold positions other than the hinge area, such as within the limbs or the hydrothermal corridor representing the zone delimited by the Campbell and Dickenson faults (*see* Dubé et al., 2001a, Fig. 1), thus in areas where layer-parallel extension of competent layers in the fold hinges cannot be as easily invoked. Figures 1b and 1c show that in the Goldcorp High Grade zone, the poles of foliation and veins fall on a great circle with a pole corresponding to the axes of folds deforming the veins. This distribution of poles is not solely the product of folding of the main S_2 fabric and subparallel veins, as it may appear at first glance. Although it is partly due to folded veins, it largely reflects the presence of several vein sets intersecting along a line parallel to F_{2b} fold axes, as illustrated by maxima on the stereonets (Fig. 1c) and as recognized elsewhere in the deposit by Rogers (1992) and Zhang et al. (1997). Although the original vein geometry has been modified by continuous deformation, the three main sets of carbonate veins are interpreted to form a broadly contemporaneous, three-dimensional network with the southeast set being by far the best developed. This vein network developed mainly during the same deformation increment, as suggested by the identical hydrothermal

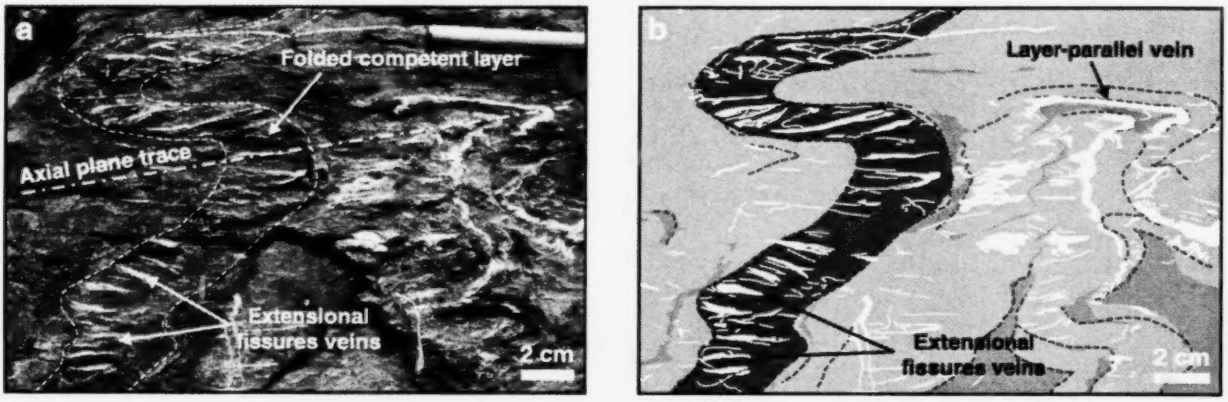

Figure 6. *a) Small-scale example of vein distribution controlled by layer-parallel stretching of a folded (F_2) stiff layer, with thicker extensional fissure veins in the outer arc and at a high angle to the folded competent layer and buckled bedding-parallel veins along the competent–incompetent interface, plane view;* ***b****) sketch of* ***a****.*

	D_1	D_2		
		D_{2a}	D_{2b}	D_{2c} / D_3 (?)
N-S-trending F_1 open folds				
Carbonate veins network	? — ?			
ESE F_{2a} folds deforming lithology				
ESE trending S_2 main foliation				
Carbonate veins boudinage				
Biotite alteration				
Au-rich silica and arsenopyrite replacement				
SW F_{2b} folds deforming veins				
ESE-trending high strain / shear zones				
SW-plunging L_{2b} stretching lineation				
ESE reverse-sinistral brittle-ductile faulting				
FP dykes				
Lamprophyre dykes				
Barren quartz veins				
Au remobilization				

Figure 7. *Relative chronology of the main geological features.*

characteristics. Figure 1c shows a common intersection of veins and host structures oriented approximately 271°/48° (Fig. 1e). It is assumed that this orientation defines the bulk intermediate axis of incremental strain (Y_{2a}) recorded by the development of the vein network (Fig. 1e). The common intersection of veins is also parallel to the elongation lineation (X_{2b}) defined by the stretching lineation. The two are kinematically incompatible because the intermediate incremental strain axis defined by the vein network (Y_{2a}) should be perpendicular to its elongation axis (X_{2a}) associated with the S_2 foliation, and not parallel to it (Fig. 1e). Therefore, D_{2b} should be separated from D_{2a}. For this reason and on the basis of relative chronology, at least three distinct strain increments or structure generations regionally attributed to D_2 must have occured (Fig. 7). 1) Northeast-southwest-directed shortening accounts for the folding of the east-trending Balmer assemblage by F_{2a} folds and the formation of the axial-planar fissure veins, the discordant sets of veins along the limbs, and the locally developed bedding-parallel vein structures (Fig. 8a). This shortening may also have caused oblique ((?)sinistral) displacement along the incipient Campbell, Dickenson, and other southeast-trending faults. The subsidiary, brittle-ductile, east-west and south-southeast structures, such as HW5, would then represent discordant ((?)conjugate) structures oriented 60° to one another. This would be compatible with their intersection at high angle to the F_{2a} fold axes. During this early increment of D_2 strain, local higher strain zones may also have developed along east-trending lithological contacts, such as the 'east-west shear', along the fold limbs due to contrasting competence, and along extensional veins parallel to the northeast-southwest-oriented axis of shortening. 2) During and following the formation of the vein

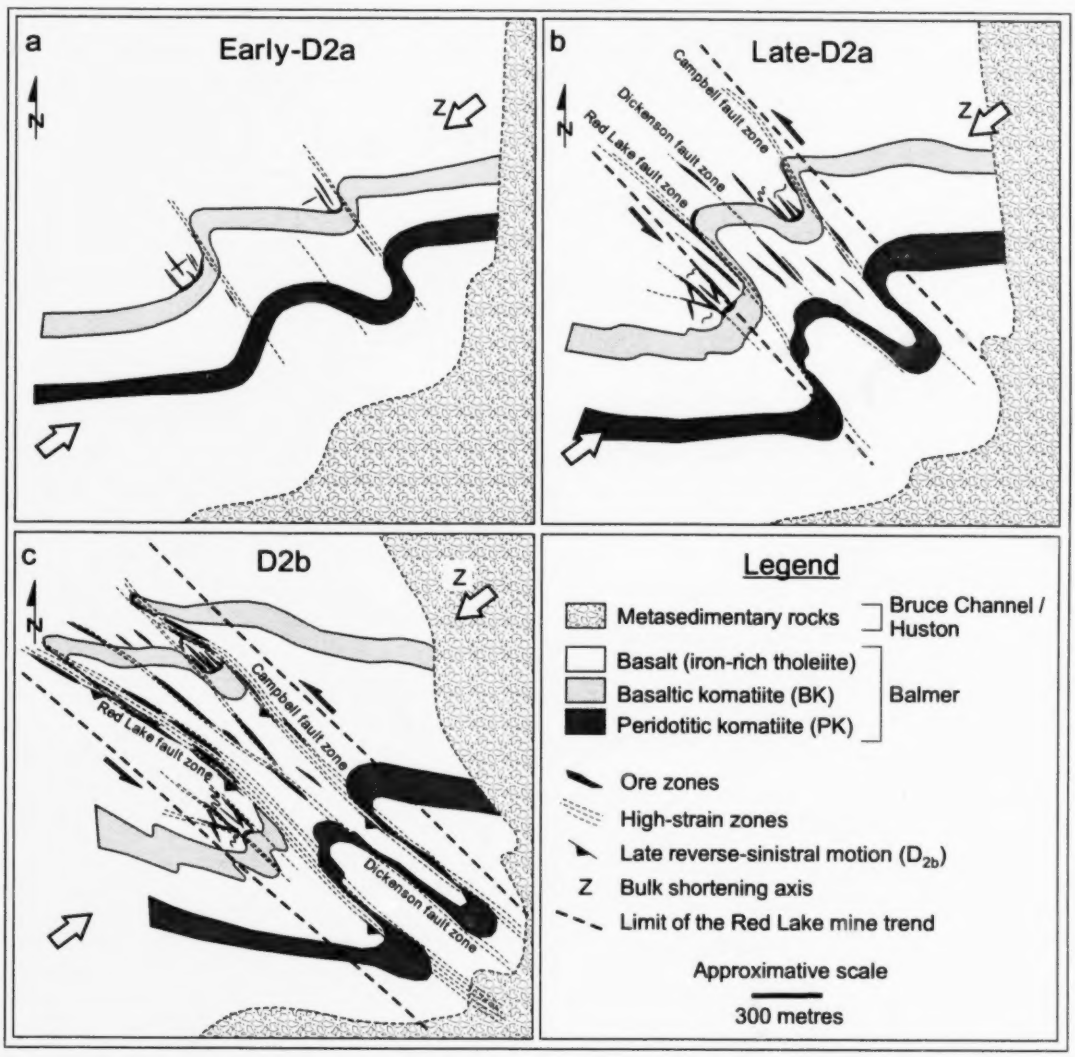

Figure 8. *Schematic evolution model of the Campbell-Red Lake deposit relative to D_2 deformation, based on a geological compilation by Goldcorp Inc. and Dubé et al. (2001a).*

network and F_{2a} folds, continuous northeast-southwest shortening induced a second strain increment characterized by tightening of the F_{2a} folds and transposition of their limbs (Fig. 8b). This enhanced the axial-planar S_2 foliation, formed southeast high-strain zones, and initiated or enhanced foliation in the east-west and south-southeast higher strain zones as a result of strain refraction due to contrasting competence induced by the rigid carbonate vein. The strain was accommodated by the host basalt along the vein contacts. Continuous shortening also induced deformation of the vein network particularly the south-southeast-trending breccia veins that were folded, transposed, and boudinaged by S_2. The asymmetry of the F_{2a} folds and the geometry of the asymmetrical boudins deforming the carbonate veins are compatible with a reverse component of motion and with moderate to steep extension recorded by L_2. Ultimately, the strain was accommodated by shearing and faulting of the limbs and generated structures such as the Campbell and Red Lake faults (Fig. 8c). This generation of D_2 structures would be associated with the reverse-sinistral motion recorded by the Campbell Fault. The Campbell Fault plane mapped is barren and probably represents the last stages of this deformation increment; it postdates auriferous silicic replacement. 3) The en échelon barren quartz veins hosted by the lamprophyre dykes are at a high angle to the L_2 stretching lineations; they indicate that vertical stretching outlasted the mineralized hydrothermal system and that the lamprophyre records a third increment of D_2 strain (D_{2c} or D_3) with similar subvertical extension.

Regardless to their orientation, most carbonate veins show internal features typical of extensional or cavity-fill veins with colloform-crustiform-cockade texture and locally fibres at high angle to vein walls. The presence of a foliation parallel to these extensional veins is a structural anomaly recognized within the deposit by MacGeehan and Hodgson (1982), Penczak and Mason (1997), and Dubé et al. (2001a). These Fe-carbonate veins show strong similarities with the auriferous concordant ankerite veins at the Dome mine in terms of nature, structural setting, and spatial relationship to folding and to an unconformity. However, nowhere are the colloform-crustiform textures better developed in Archean gold deposits than at the Campbell-Red Lake deposit. On the basis of chronology and geometry of structures developed during the first increment of D_2 strain and despite the presence of a foliation parallel to these veins in the host, extreme fluid pressure may have been a key factor influencing the higher rate of dilation than crystal growth needed to form the colloform-crustiform, cavity-fill texture in the vein (e.g. Foxford et al., 1991).

Alternatively, the carbonate vein network could predate D_2 deformation and be related to D_1, as suggested by the overprinting fabrics. This would explain why many veins are deformed by F_2 folds, why the carbonate vein network is incompatible with L_2, and why S_2 is subparallel to these extensional veins. D_1 is characterized by east-trending shortening (Sanborn-Barrie et al., 2001), which is not incompatible with the geometry of the extensional network of carbonate veins. In such a D_1 model, the carbonate veins could be of low-sulphidation epithermal origin, as proposed by Penczak and Mason (1997). However, this would imply that they are

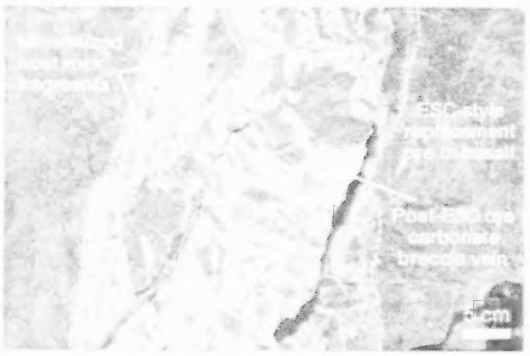

Figure 9. *Carbonate breccia vein postdating ESC replacement mineralization, section view; stope 16-01-7.*

spatially related to the ore zones and the Red Lake mine trend, but separated in time and genesis from the syn-D_2 auriferous hydrothermal event. This scenario is unlikely as auriferous ESC replacement mineralization (level 16, stope 16-01-7) is locally cut by barren carbonate breccia veins with typical cockade texture (Fig. 9) (Dubé et al., 2001a), unless several generations of similar carbonate veining occur.

The relative chronology suggests that auriferous silicic carbonate-vein replacement occurred during D_2-related asymmetrical boudinage of the veins. The geometry of the boudins suggests that boudinage occurred late during the first increment of D_2 strain, or early during the second increment of D_2 strain, which is characterized by a reverse-sinistral component of motion.

Emplacement of the 2699 Ga Walsh Lake Pluton east of the deposit (e.g. Sanborn-Barrie et al., 2001) may have played a key role in the mineralization as originally proposed by Andrews et al. (1986). The pluton and the Trout Lake batholith that it surrounds most probably represent the end products of a large-scale thermal front with a protracted history of uplift and structural, thermal, and hydrothermal (?)gold-bearing) disturbances most likely much older than the age of pluton crystallization, which may explain the diachronism and conflicting chronology (*see also* Parker, 2000) of magmatism, metamorphism, deformation, and gold mineralization and remobilization.

CONCLUSIONS

The main stage of high-grade, Au-rich silica was contemporaneous with the D_2 boudinage of carbonate veins. Gold mineralization is synchronous with D_2 shortening, a protracted event characterized mainly by continuous shortening that caused folding of a layered sequence and synchronous emplacement of axial-planar fissure veins as well as bedding-parallel and discordant (?conjugate) veins, followed by attenuation and transposition of the limbs and ultimately reverse-sinistral faulting. The F_{2a} fold hinges deforming the basalt–basaltic komatiite contact control the distribution of the high-grade gold mineralization. The auriferous silica-rich fluid was focused into these lower pressure F_{2a} hinge zones as

network and F_{2a} folds, continuous northeast-southwest shortening induced a second strain increment characterized by tightening of the F_{2a} folds and transposition of their limbs (Fig. 8b). This enhanced the axial-planar S_2 foliation, formed southeast high-strain zones, and initiated or enhanced foliation in the east-west and south-southeast higher strain zones as a result of strain refraction due to contrasting competence induced by the rigid carbonate vein. The strain was accommodated by the host basalt along the vein contacts. Continuous shortening also induced deformation of the vein network particularly the south-southeast-trending breccia veins that were folded, transposed, and boudinaged by S_2. The asymmetry of the F_{2b} folds and the geometry of the asymmetrical boudins deforming the carbonate veins are compatible with a reverse component of motion and with moderate to steep extension recorded by L_2. Ultimately, the strain was accommodated by shearing and faulting of the limbs and generated structures such as the Campbell and Red Lake faults (Fig. 8c). This generation of D_2 structures would be associated with the reverse-sinistral motion recorded by the Campbell Fault. The Campbell Fault plane mapped is barren and probably represents the last stages of this deformation increment; it postdates auriferous silicic replacement. 3) The en échelon barren quartz veins hosted by the lamprophyre dykes are at a high angle to the L_2 stretching lineations; they indicate that vertical stretching outlasted the mineralized hydrothermal system and that the lamprophyre records a third increment of D_2 strain (D_{2c} or D_3) with similar subvertical extension.

Regardless to their orientation, most carbonate veins show internal features typical of extensional or cavity-fill veins with colloform-crustiform-cockade texture and locally fibres at high angle to vein walls. The presence of a foliation parallel to these extensional veins is a structural anomaly recognized within the deposit by MacGeehan and Hodgson (1982), Penczak and Mason (1997), and Dubé et al. (2001a). These Fe-carbonate veins show strong similarities with the auriferous concordant ankerite veins at the Dome mine in terms of nature, structural setting, and spatial relationship to folding and to an unconformity. However, nowhere are the colloform-crustiform textures better developed in Archean gold deposits than at the Campbell-Red Lake deposit. On the basis of chronology and geometry of structures developed during the first increment of D_2 strain and despite the presence of a foliation parallel to these veins in the host, extreme fluid pressure may have been a key factor influencing the higher rate of dilation than crystal growth needed to form the colloform-crustiform, cavity-fill texture in the vein (e.g. Foxford et al., 1991).

Alternatively, the carbonate vein network could predate D_2 deformation and be related to D_1, as suggested by the overprinting fabrics. This would explain why many veins are deformed by F_2 folds, why the carbonate vein network is incompatible with L_2, and why S_2 is subparallel to these extensional veins. D_1 is characterized by east-trending shortening (Sanborn-Barrie et al., 2001), which is not incompatible with the geometry of the extensional network of carbonate veins. In such a D_1 model, the carbonate veins could be of low-sulphidation epithermal origin, as proposed by Penczak and Mason (1997). However, this would imply that they are

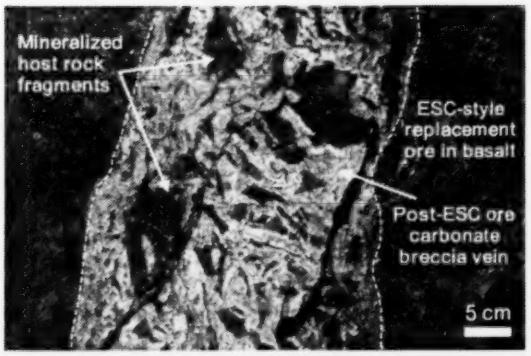

Figure 9. *Carbonate breccia vein postdating ESC replacement mineralization, section view; stope 16-01-7.*

spatially related to the ore zones and the Red Lake mine trend, but separated in time and genesis from the syn-D_2 auriferous hydrothermal event. This scenario is unlikely as auriferous ESC replacement mineralization (level 16, stope 16-01-7) is locally cut by barren carbonate breccia veins with typical cockade texture (Fig. 9) (Dubé et al., 2001a), unless several generations of similar carbonate veining occur.

The relative chronology suggests that auriferous silicic carbonate-vein replacement occurred during D_2-related asymmetrical boudinage of the veins. The geometry of the boudins suggests that boudinage occurred late during the first increment of D_2 strain, or early during the second increment of D_2 strain, which is characterized by a reverse-sinistral component of motion.

Emplacement of the 2699 Ga Walsh Lake Pluton east of the deposit (e.g. Sanborn-Barrie et al., 2001) may have played a key role in the mineralization as originally proposed by Andrews et al. (1986). The pluton and the Trout Lake batholith that it surrounds most probably represent the end products of a large-scale thermal front with a protracted history of uplift and structural, thermal, and hydrothermal ((?)gold-bearing) disturbances most likely much older than the age of pluton crystallization, which may explain the diachronism and conflicting chronology (*see also* Parker, 2000) of magmatism, metamorphism, deformation, and gold mineralization and remobilization.

CONCLUSIONS

The main stage of high-grade, Au-rich silica was contemporaneous with the D_2 boudinage of carbonate veins. Gold mineralization is synchronous with D_2 shortening, a protracted event characterized mainly by continuous shortening that caused folding of a layered sequence and synchronous emplacement of axial-planar fissure veins as well as bedding-parallel and discordant ((?)conjugate) veins, followed by attenuation and transposition of the limbs and ultimately reverse-sinistral faulting. The F_{2a} fold hinges deforming the basalt–basaltic komatiite contact control the distribution of the high-grade gold mineralization. The auriferous silica-rich fluid was focused into these lower pressure F_{2a} hinge zones as

a result of a combination of factors including competence contrasts, tangential longitudinal strain, and southeast-trending high-strain zones. The barren carbonate vein network is related to the early D_{2a} strain increment, but the possibility that some veins predate D_2 can not be ruled out entirely.

The geometry of the vein network and the F_{2a} fold deforming the basalt–basaltic komatiite contact is related to an early D_{2a} strain increment caused by northeast-southwest-directed shortening, which caused folding of the mine sequence and possibly some oblique ((?)sinistral) displacement, both of which were involved in the formation of the carbonate vein network and the auriferous silicic replacement. Such an evolution shares some analogies with N. Archibald and V. Wall, unpub. rept., 2001. This was followed by a second strain increment (D_{2b}) with reverse-sinistral motion.

The Red Lake district is characterized by high gold endowment; however, the average grade of 88 g/t Au mined in the Goldcorp Inc. High Grade zone is too high to be solely the product of such a heritage. The structural location of the zone in an F_{2a} hinge is one of the main differences between ore at ~15 g/t Au, such as in the ESC zones, and the high-grade ore in the High Grade zone. The extremely high gold values result from a combination of factors, including the following:

1. the F_{2a} fold hinges deforming the basalt and basaltic komatiite contact, which played a key role in the formation of the veins network;
2. the basaltic komatiite located structurally above the basalt in the F_{2a} antiform, which acted as a low-permeability cap controlling fluid migration and allowing the buildup of very high fluid pressure and an extreme fluid–rock ratio in the hinge zone, resulting in a ponding effect in the basalt and the creation of high-grade ore within the lower pressure F_{2a} fold hinge;
3. a CO_2-rich hydrothermal stage followed by auriferous syn-D_2 silicic replacement;
4. the iron-rich content of the tholeiitic basalt that allowed precipitation of arsenopyrite and gold by reaction with the fluids, with the more competent basalt acting as a chemical and structural trap for the fluids and constituting the 'ore horizon';
5. several increments of D_2 strain with high-grade gold deposited during D_2 and locally remobilized in extremely rich fractures that postdate emplacement of the lamprophyre dykes.

ACKNOWLEDGMENTS

Goldcorp Inc. and in particular Gilles Filion, Stephen McGibbon, Tim Twomey, Rob Penczak, John Kovala, Michael Collins, Mark Epp, Matt Ball, Michael Dehn, and the entire production staff at the mine are thanked for their scientific contribution, logistic and financial support, critical review, and permission to publish. Mary Sanborn-Barrie, Tom Skulski, Jack Parker, Vic Wall, and Nick Archibald are thanked for constructive discussions in the field. Placer Dome is sincerely thanked for underground visits at the Campbell mine and for sharing its knowledge. Critical review by Alain Tremblay improved the manuscript.

REFERENCES

Andrews, A.J., Hugon, H., Durocher, M., Corfu, F., and Lavigne, M.
1986: The anatomy of a gold-bearing greenstone belt: Red Lake, northwestern Ontario; Gold '86 Symposium, Toronto, p. 3–22.

Damer, G.C.
1997: Metamorphism of hydrothermal alteration at the Red Lake Mine, Balmertown, Ontario; M.Sc. thesis, Queen's University, Kingston, Ontario, 195 p.

Dubé, B., Williamson, K., and Malo, M.
2001a: Preliminary report on the geology and controlling parameters of the Goldcorp Inc. High Grade zone, Red Lake mine, Ontario; Geological Survey of Canada, Current Research 2001-C18.
2001b: The Goldcorp high-grade zone, Red Lake mine, Ontario: a photographic atlas of the main geological features; Geological Survey of Canada, Open File 3890.

Foxford, K., Nicholson, R., and Polya, D.
1991: Textural evolution of W-Cu-Sn-bearing hydrothermal veins at Minas da Panasqueira, Portugal; Mineralogical Magazine, v. 55, p. 435–445.

Mathieson, N.A.
1982: Geology and mineralization in the area of the East South "C" ore zone, Dickenson mine, Red lake district, northwestern Ontario; M.Sc. thesis, Queen's University, Kingston, Ontario, 155 p.

MacGeehan, P. and Hodgson, C.J.
1982: Environments of gold mineralization in the Campbell-Red Lake and Dickenson mines, Red Lake district, Ontario; *in* Geology of Canadian Gold Deposits; Canadian Institute of Mining and Metallurgy, Special Volume 24, p. 184–207.

Parker, J.R.
2000: Gold mineralization and wall-rock alteration in the Red Lake greenstone belt: a regional perspective; *in* Summary of Field Work and Other Activities; Ontario Geological Survey, Open File Report 6032, p. 22-1–22-28.

Penczak, R. and Mason, R.
1997: Metamorphosed Archean epithermal Au-As-Sb-Zn-(Hg) vein mineralization at the Campbell mine, northwestern Ontario; Economic Geology, v. 92, p. 696–719.
1999: Characteristics and origin of Archean premetamorphic hydrothermal alteration at the Campbell gold mine, northwestern Ontario, Canada; Economic Geology, v. 94, p. 507-528.

Rogers, J.
1992: The Arthur W White mine, Red Lake area, Ontario: detailed structural interpretation, the key to successful grade control and exploration; CIM Bulletin 85, no. 957, p. 37–44.

Sanborn-Barrie, M., Skulski, T., Parker, J., and Dubé, B.
2000: Integrated regional analysis of the Red Lake belt and its mineral deposits, western Superior Province, Ontario; Geological Survey of Canada, Current Research 2000-C18.

Sanborn-Barrie, M., Skulski, T., and Parker, J.
2001: Three hundred million years of tectonic history recorded by the Red Lake greenstone belt, Ontario; Geological Survey of Canada, Current Research 2001-C19.

Zhang, G., Hattori, K., and Cruden, A.
1997: Structural evolution of auriferous deformation zones at the Campbell mine, Red lake geenstone belt, Superior Province; Precambrian Research, v. 84, p. 83–103.

Geological Survey of Canada Project PS2011